Ion channel properties underlying axonal action potential initiation in pyramidal neurons

Costa M. Colbert and Enhui Pan

Department of Biology and Biochemistry, University of Houston, 4800 Calhoun Road, Houston, Texas 77204-5513, USA
Correspondence should be addressed to C.C. (ccolbert@uh.edu)

Published online: 6 May 2002, DOI: 10.1038/nn857

A high density of Na^+ channels in the axon hillock, or initial segment, is believed to determine the threshold for action potential initiation in neurons. Here we report evidence for an alternative mechanism that lowers the threshold in the axon. We investigated properties and distributions of ion channels in outside-out patches from axons and somata of layer 5 pyramidal neurons in rat neocortical slices. Na^+ channels in axonal patches (>30 μm from the soma) were activated by 7 mV less depolarization than were somatic Na^+ channels. A-type K^+ channels, which were prominent in somatic and dendritic patches, were rarely seen in axonal patches. We incorporated these findings into numerical simulations which indicate that biophysical properties of axonal channels, rather than a high density of channels in the initial segment, are most likely to determine the lowest threshold for action potential initiation.

Determining where and when action potentials originate is critical to understanding the computations that neurons perform[1–3]. A precise definition of the conditions for action potential initiation requires knowledge of the distribution and of the biophysical properties of the underlying ion channels. Because of the very small diameters of axons in the brain, direct electrophysiological measurements of axonal ion channels have only recently become feasible. Thus, the determinants of threshold and the site of initiation of action potentials in cortical neurons have remained a subject of debate[4,5].

Considerable recent evidence indicates that action potentials are often initiated near the soma rather than at the site of synaptic input in the dendrites[6–14], suggesting that the axon has a low threshold for action potential initiation. The mechanism underlying this low threshold has long been assumed to be a high density of Na^+ channels in the axon hillock or initial segment, which is typically 25–30 μm in length as defined by ultrastructural characteristics[15,16]. Although such a mechanism receives support from theoretical studies[14,17–19] and from labeling studies[20–22], electrophysiological studies of action potential initiation in large pyramidal neurons indicate that the initial segment is not the site of action potential initiation in these cells. First, simultaneous recordings from the soma and initial segment indicate that action potentials are initiated in the axon beyond the initial segment in response to synaptic input in layer 1 (ref. 10). Second, local application of tetrodotoxin (a Na^+ channel blocker) to the initial segment does not alter the threshold for initiating action potentials in response to somatic current injection. Instead, application of tetrodotoxin to the axon beyond the initial segment raises the threshold by 7–10 mV (ref. 23). These results indicate that Na^+ channels in the axon proper rather than in the initial segment may determine the threshold.

With these data in mind, we investigated biophysical mechanisms that might contribute to a low threshold for action potential initiation in the axon. We recorded currents from membrane patches in somata, initial segments and axons of layer 5 pyramidal neurons in rat neocortical slices. There was a difference in the voltage dependence of activation of Na^+ channels across these regions that favors the initiation of action potentials in the axon. We also found that A-type K^+ channels, which were prominent in somatic patches, were only rarely present in patches from the axon or initial segment.

Results

We measured currents using the outside-out patch configuration, which provided several advantages over other recording modes for our specific experiments. First, because we recorded briefly in the whole-cell configuration before the patch was pulled, we could assess the health of the cell before forming the patch. Second, we could ensure that the electrode was attached to neuronal rather than glial membrane by evoking an action potential. Third, the voltage clamp directly set the transmembrane potential, thus minimizing errors in estimating the resting potential of the neuron. We recorded currents in visually identified somata (**Fig. 1a**), in initial segments (<30 μm from the soma) and in axons (30–47 μm from the soma).

The set of currents evoked by depolarizing steps from a negative holding potential differed qualitatively between axonal and somatodendritic patches. In somatic patches (**Fig. 1b**) and in patches from the basal dendrites (not shown, $n = 4$), a rapidly activating and inactivating inward current (I_{Na}) was followed by an outward current with both transient ($I_{K(A)}$, A-type) and sustained ($I_{K(DR)}$, delayed rectifier) components[9,23,24]. In patches from the initial segment and axon proper, however, A-type

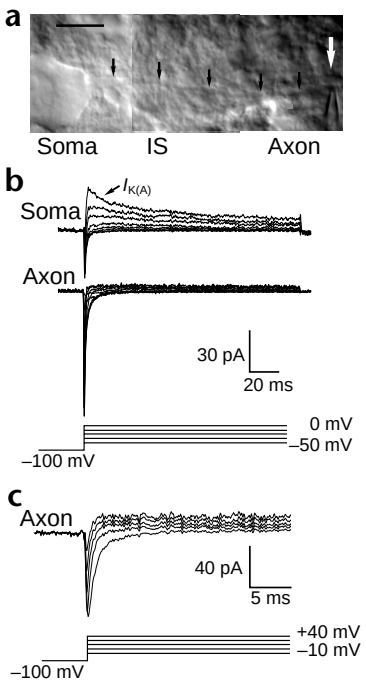

Fig. 1. Total ensemble currents in outside-out patches from visually identified somata and axons of neocortical layer 5 pyramidal neurons. (**a**) Infrared-illuminated, differential interference contrast image of a pyramidal neuron. Small arrows indicate the path of an axon. White arrow indicates the recording electrode. IS, initial segment. Scale bar, 10 μm. (**b**) Representative currents in outside-out patches from the soma and axon. Patches were held at a holding potential of –100 mV and stepped to test potentials between –50 and 0 mV. Somatic patches had a prominent transient outward current ($I_{K(A)}$) in addition to inward I_{Na} and sustained outward $I_{K(DR)}$ currents. Axonal patches did not have the transient outward current. (**c**) In axonal patches, applying greater depolarizations (–10 to 40 mV) to increase the driving force of K^+ currents did not result in any transient K^+ currents. Waveforms are leak-subtracted averages of 15–20 individual sweeps.

current was only occasionally seen (2 of 18 patches). This may have resulted from either a low density of A-type channels or a restriction of these channels to specific regions[25]. In most patches, only the inward and the sustained outward currents were present (**Fig. 1b** and **c**). Tetrodotoxin (1 μM) blocked the inward current ($n = 2$) and 10 mM tetraethylammonium blocked the sustained outward current, as expected for I_{Na} and $I_{K(DR)}$.

To test whether the biophysical properties and distribution of Na^+ channels varied in the soma, initial segment and axon, we compared ensemble averages of Na^+ currents (**Fig. 2a**). We constructed an activation curve from each ensemble and fit it with a Boltzmann curve (**Fig. 2b**, see Methods) to yield a half-activation potential ($V_{1/2}$) and a slope (k). Patches from the somata, initial segments and axons had $V_{1/2}$ values of –31.6 ± 0.5 mV ($n = 7$), –30.1 ± 1.4 mV ($n = 7$) and –38.4 ± 1.6 mV ($n = 8$) and k values of 6.8 ± 0.46 ($n = 7$), 8.1 ± 0.62 ($n = 7$) and 6.0 ± 0.48 ($n = 8$), respectively. A one-way analysis of variance (ANOVA) of the half-activation potentials indicated significant differences between the axon and soma and between the axon and initial segment. A plot of $V_{1/2}$ as a function of the distance from the soma indicated that this may have been due to a shift in the voltage dependence near the end of the initial segment rather than a gradual decrease with distance (**Fig. 2c**). Thus, Na^+ channels in the axon proper required less depolarization for activation than did Na^+ channels in the soma or initial segment.

Next, we estimated the relative density of Na^+ channels by comparing the magnitude of peak currents in somatic and axonal patches. Patches from the somata, initial segments and axons had peak currents of 26.6 ± 7.9 pA ($n = 8$), 22.4 ± 0.5 pA ($n = 7$) and 99.8 ± 33.7 pA ($n = 9$). Excluding a single outlier in the axon group of 308 pA reduced the peak current to 63.9 ± 13.0 pA ($n = 8$). Plotting the peak current versus distance from the soma (**Fig. 2d**) indicated that the current per patch was uniform throughout the initial segment before increasing two- to threefold in the axon. Steady-state inactivation, however, was similar in all patches. (Half-inactivation potentials for soma, initial segment and axon were –66 ± 2.4 mV ($n = 6$), –66 ± 1.8 mV ($n = 5$) and –69 ± 1.2 mV ($n = 5$) and slopes were 5.3 ± 0.6 ($n = 6$), 5.9 ± 1.8 ($n = 5$) and 5.3 ± 0.8 mV ($n = 5$), respectively.)

Previous work addressing action potential initiation in pyramidal neurons indicated that there may be a 7–10-mV difference in the voltage thresholds of the axon and soma[23]. To investigate whether the voltage dependence of Na^+ channel activation could account for such a difference in threshold, we numerically simulated a pyramidal neuron using a compart-

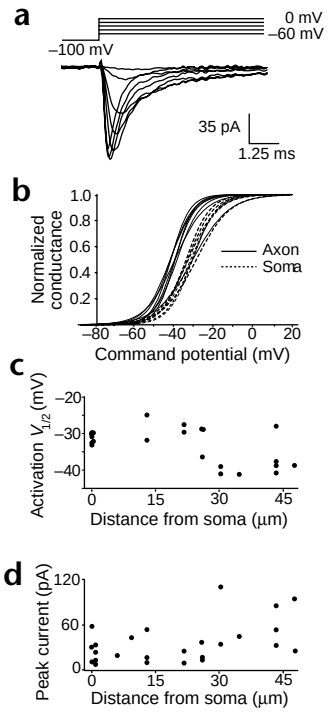

Fig. 2. Na^+ channel properties differ between the soma and axon. (**a**) Representative ensemble currents in an outside-out patch from the soma. The patch was held at a holding potential of –100 mV and stepped to test potentials from –60 to 0 mV. (**b**) Voltage dependence of activation in somatic and axonal patches. Each curve is the best-fit Boltzmann for an individual patch. Axonal Na^+ channels (solid lines) were activated by less depolarization than somatic channels (dotted lines). (**c**) $V_{1/2}$ of Na^+ currents plotted as a function of position along the axon. (**d**) Peak Na^+ current at 0 mV plotted for each patch as a function of position along the axon. The values in (**c**) and (**d**) remained relatively constant throughout the initial segment before changing in the axon.

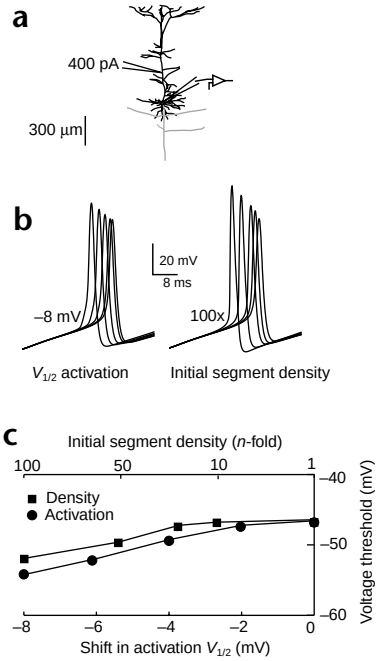

Fig. 3. Effect of Na^+ channel properties on action potential threshold: computer simulations. (**a**) Reconstructed cell showing the position of current injection (400 pA) into the apical dendrite. (**b**) Superimposed somatic action potential waveforms. Rightmost action potential in each panel corresponds to uniform $V_{1/2}$ and density. Left, the $V_{1/2}$ of Na^+ channel activation was varied from –2 to –8 mV. Right, the density of Na^+ channels in the initial segment was increased 10-, 20-, 50- and 100-fold. (**c**) Voltage thresholds measured at the soma for each value of increased density (squares) and shifted $V_{1/2}$ (circles). Although both modifications lowered the threshold, very high increases in density were required.

mental model (**Fig. 3**). We also investigated how a high density of Na^+ channels in the initial segment might alter the threshold. First, we varied the $V_{1/2}$ of Na^+ channels in the axon beyond the initial segment from –2 mV to –8 mV (**Fig. 3b**, left). The action potential threshold measured at the soma became more negative as the shift in $V_{1/2}$ became greater (**Fig. 3c**). The observed shifts in $V_{1/2}$ were sufficient to account for the differences in the experimentally observed threshold. To test the effect on the threshold of Na^+ channel density in the initial segment, we varied the density from 10- to 100-fold, as compared with the somatic density, while keeping the $V_{1/2}$ uniform (**Fig. 3b**, right). Increasing the Na^+ channel density in the initial segment decreased the threshold, but this required very high channel densities (**Fig. 3c**).

We next investigated how the site of initiation varied as a function of axonal Na^+ channel activation or initial segment density using the compartmental model. We observed the initial development of the action potential by plotting membrane potential as a function of position (a space plot) along the axon, soma and the apical dendrite (**Fig. 4a–c**) and as a function of time (**Fig. 4b**). With Na^+ channel activation held uniform across the neuron, current injection into the dendrite (350 µm from the soma, 500 pA) produced a regenerative depolarization across the neuron's initial segment and much of its somatodendritic extent (**Fig. 4a** and **b**, 0 mV). That is, the action potential was initiated simultaneously across much of the neuron rather than propagating through the neuron. Shifting the $V_{1/2}$ of Na^+ channels in the axon or increasing the density of Na^+ channels in the initial segment altered this pattern of action potential initiation; the action potential was initiated first in the axon or initial segment, respectively (**Fig. 4a**, –7 mV and 100× traces). This bias toward action potential initiation in the axon or initial segment was proportional to the magnitude of the shift in the $V_{1/2}$ (**Fig. 4c**, left traces) or the increase in density (**Fig. 4c**, right traces), indicating that sufficiently strong dendritic depolarization may overcome this bias to produce dendritic initiation[26,27].

Although both models lowered the threshold and biased the neuron away from initiating an action potential in the dendrites, the spatial patterns of action potential initiation differed considerably. When we shifted the $V_{1/2}$ of axonal Na^+ channels toward more negative potentials, the length of axon that participated in producing the regenerative current during action potential initiation (200 µm) was much greater than

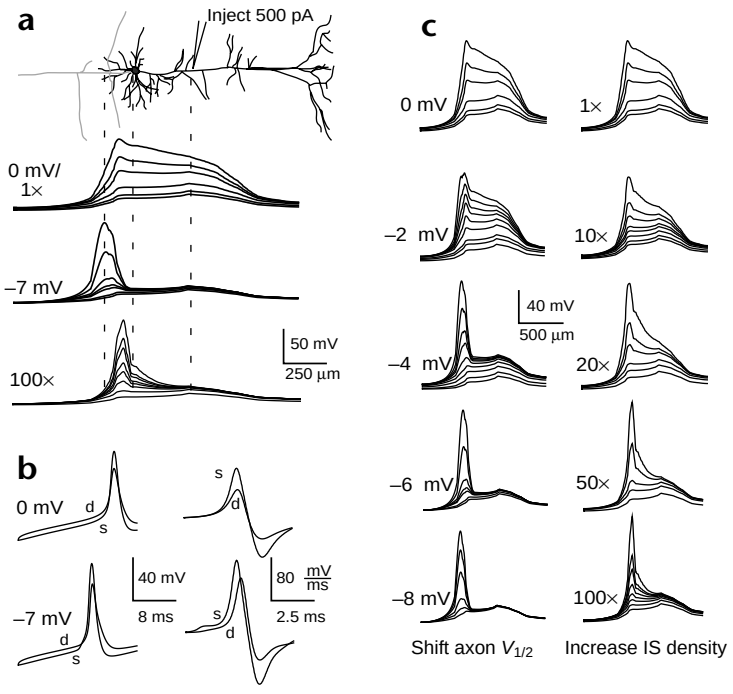

Fig. 4. Spatial patterns of action potential initiation: computer simulations. (**a**) Reconstructed cell showing the position of current injection (500 pA) into the apical dendrite (top). Space plots show membrane potential (V_m) across the axodendritic axis. Waveforms in each group represent different time points beginning just before action potential initiation and ending before propagation begins. 0 mV/1×, uniform Na^+ channel properties; –7 mV, Na^+ channel activation shifted –7 mV in the axon; 100×, 100-fold increase in Na^+ channel density in the initial segment. (**b**) Action potential waveforms (left) in the soma (s) and dendrites (d) and corresponding time derivatives d*V*/d*t* (right). 0 mV, uniform Na^+ channel properties; –7 mV, Na^+ channel activation shifted –7 mV in the axon. (**c**) Space plots as in (**a**) at intermediate values of shifted activation (left) and increased initial segment (IS) density (right).

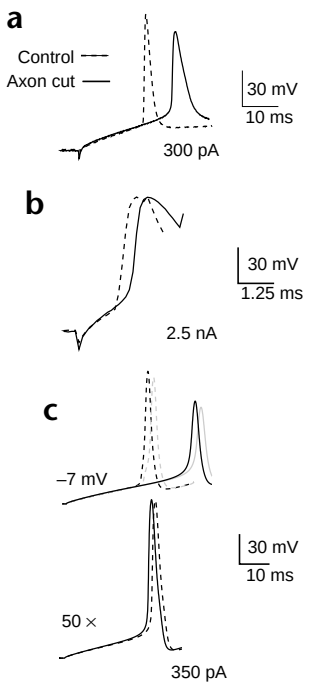

Fig. 5. Threshold increases when a pyramidal neuron is cut at the end of the initial segment. (**a**) Action potentials recorded in response to somatic current injection in a control pyramidal neuron (dotted line) and a pyramidal neuron with its axon cut at the end of the initial segment (solid line). Cutting the axon raised the threshold. (**b**) A brief strong current injection evoked a full-amplitude action potential in both the control and cut cells. (**c**) Computer simulations of cut (solid lines) and control neurons (dotted lines) distinguished between models. With a –7-mV shift in Na^+ channel activation in the axon and either uniform (black lines) or 10-fold higher (gray lines) density of Na^+ channels in the initial segment cutting the axon raised the threshold, (upper traces). With 50-fold higher density of Na^+ channels in the initial segment, cutting the axon did not raise the threshold (lower traces).

the length of the initial segment. In fact, the initial segment contributed relatively little to the regenerative current, because the electrical load presented by the soma and dendrites limited its depolarization. In contrast, in the high-Na^+-channel-density model, the initial segment played the chief role in producing the initial regenerative current. The pattern of initiation in the shifted-activation model was thus more consistent with previous experimental results where direct application of tetrodotoxin to the initial segment did not change the threshold[23].

The fortuitous finding of a pyramidal neuron that had been cut through the axon at 25 μm from the soma by the slicing procedure allowed a further experimental test of the models. We compared thresholds in this cut neuron and in a neighboring pyramidal neuron (in the same field in the slice) that did not have a cut axon. Both cells were healthy by visual criteria and had resting potentials of –63 mV. The shifted-Na^+-channel-activation model predicted that cutting the axon at the end of the initial segment would raise the threshold because the cut would eliminate the channels with shifted activation. The high-density model predicted that threshold would not increase because the cut would preserve the high density of channels in the initial segment. Recording from the neuron with the cut axon showed an increased threshold in response to somatic depolarization (**Fig. 5a**). The action potential was also greatly reduced in amplitude and rate. To test whether the small amplitude of the action potential in the cut neuron was due to inactivation of Na^+ channels or was an indication of some other damage, we stimulated each neuron with a strong depolarizing current. The resulting action potentials in each neuron had equivalent amplitude and rate of rise (**Fig. 5b**), indicating that no substantial source of Na^+ current near the soma was lost because of the cut. Numerical simulation confirmed that cutting the axon at the end of the initial segment raised the threshold in the shifted-activation model but not in the high-density model (**Fig. 5c**).

Discussion

These data are the first direct electrophysiological measurements in cortical axons of ion channel properties and distributions that contribute to a low threshold for action potential initiation. They imply a mechanism favoring initiation of action potentials in the axon that differs in two ways from the widely accepted scheme. First, the properties of Na^+ channels producing the low threshold for action potential initiation exist in the axon proper rather than in the axon hillock/initial segment. A long history of reports indicating that action potential initiation may occur beyond the axon hillock/initial segment[10,23,28–31] substantiates this idea. Second, a shift in the voltage dependence of activation of Na^+ channels in the axon, rather than a high density of Na^+ channels in the initial segment, determines the low threshold. In addition to the present findings, rapid changes in threshold after the induction of long-term potentiation[32] and after pharmacological activation of protein kinase C (ref. 33) seem more readily explained by modulation of channel properties than by rapid insertion of large numbers of Na^+ channels into the membrane.

Although it has been commonly believed that a high density of Na^+ channels in the axon hillock and initial segment determines the threshold for action potential initiation, this idea has had mixed experimental support. A high density was apparently first suggested in a computer study[17] motivated by ultrastructural similarities between the node of Ranvier and the initial segment[15,16]. Subsequent immunohistochemical studies[20,21] indicated that there may be as much as a tenfold higher density of Na^+ channels in the initial segment, although only a fraction of neurons showed increased densities. A freeze-fracture study found the total number of particles in the initial segment to be only threefold higher than in the soma[34]. Patch-clamp studies in subiculum[23] and in neocortex (ref. 35 and present results) have not detected any increase in the density of Na^+ channels in the initial segment. Of course, each of these methods may have underestimated or overestimated the true relative density of functional channels.

Recent computer simulations of pyramidal neurons used very high densities of Na^+ channels in the initial segment (200–1,000-fold higher than the somatic density) to account for the pattern of axonal action potential initiation and back-propagation in pyramidal neurons[18,19]. Together with the present simulations, the results of these studies indicate that the threshold may be relatively insensitive to Na^+ channel density in the initial segment and that moderately elevated densities such as those reported by immunohistochemical studies are unlikely to contribute strongly to a lower threshold. The relatively small effects on the threshold of altering the density of Na^+ channels in the initial segment results from morphological factors. The initial segment is physically and electrically very near the much larger soma and apical dendrite. Thus, the membrane potential of the initial segment tends to be 'clamped' to the somatic potential by the soma's relatively large capacitance. When action potentials were initiated in the axon because of the shifted $V_{1/2}$, a relatively large length of axon, as compared with the

initial segment, participated in the production of the regenerative potential. The initial segment contributed little to the depolarization but served to isolate the axon from the electrical load of the soma. The exact length of the axon that participated in initiating the action potential depended on the passive membrane parameters, which have not been explicitly determined for the small axons that we studied. Using typical ranges of values for passive parameters, however, this length was about 200–300 μm. In this case, it is more correct to think of a region of initiation rather than a discrete site. In myelinated axons, this region of initiation may be much longer and may involve multiple nodes of Ranvier. Such a finding was suggested in a study *in vivo* that compared orthodromic and antidromic action potentials in a motor neuron[31].

We have investigated two distinct models that might account for a low threshold for action potential initiation in the axon. The shifted-activation model used uniform densities, whereas the increased-density model used uniform activation. The presence or absence of these specializations need not, however, be mutually exclusive. In fact, modestly increased densities of Na^+ channels in the initial segment improved the initial rate of rise of the action potential in the simulations without much effect on the threshold (for example, **Fig. 5c**). This finding indicated that a possible role for increased density of Na^+ channels in the initial segment may be to ensure back-propagation of action potentials into the soma after initiation in the axon. Furthermore, if a high density of Na^+ channels indeed exists beyond 30 μm from the soma (despite our patch estimates), then the shifted kinetics and density would combine to lower the threshold farther, perhaps confining initiation of the action potential to this region.

A shift in the voltage dependence of activation of Na^+ channels is just one of several regional specializations within the cell that together would promote action potential initiation in the axon. A prominent gradient in the density of A-type channels in the dendrites of CA1 pyramidal neurons serves to limit dendritic initiation of action potentials[9,26]. A similar gradient of nonspecific cation channels (I_h) may function similarly by decreasing the input resistance of the dendrites[36]. Our finding that A-type K^+ channels were generally absent in axonal patches would contribute to a lower threshold in the axon. Alternatively, this finding may simply reflect the clustering of channels to perinodal regions[25].

Taken together, the presence of these specializations indicates that at least under some conditions, pyramidal neurons may be biased to initiate action potentials from an axonal site. Under such conditions, synaptic input throughout the dendrites would be summed and thresholded to produce an output in the form of an action potential in the axon, which would subsequently back-propagate into the dendrites to signal that firing has occurred[35,37]. Advantages to placing the thresholding function in the axon may include minimizing any effects of changes in dendritic or somatic conductance, or synchronizing the output of a population of neurons[38,39].

Methods

Neocortical slices (300 μm) were prepared from 14–24-day-old Sprague-Dawley rats[23] according to protocols approved by the University of Houston Institutional Animal and Use Committee. The external artificial cerebrospinal fluid contained 125 mM NaCl, 2.5 mM KCl, 1.25 mM NaH_2PO_4, 25 mM $NaHCO_3$, 2.0 mM $CaCl_2$, 1.0 mM $MgCl_2$ and 25 mM dextrose. The pipette solution used for outside-out patch recordings contained 140 mM potassium gluconate, 10 mM HEPES, 10 mM EGTA, 4.0 mM NaCl, 4.0 mM Mg_2ATP and 0.3 mM Mg_2GTP (pH 7.3). To block K^+ channels, 10 mM tetraethylammonium chloride and 10 mM 4-aminopyridine replaced equi-osmolar amounts of potassium gluconate. We included 1 μM tetrodotoxin (Alomone Labs, Jerusalem, Israel) in the bath solution to block Na^+ currents in some experiments. We purchased all other reagents from Sigma.

We visualized axons of layer 5 pyramidal neurons using infrared-illuminated differential interference contrast optics (BX50WI microscope, Olympus) and a Newvicon camera (DAGE-MTI, Michigan City, Indiana). In the oldest animals, axons beyond the initial segment looked much like those in myelinated tracts, having a 'railroad track' appearance. Whole-cell recording always yielded a cell that could fire an action potential. We made recordings using an Axopatch 200 amplifier (Axon Instruments, Union City, California) using patch pipettes of about 15 MΩ made from EN-1 glass and coated with Sylgard (Dow-Corning, Auburn, Michigan). We made all recordings at room temperature (23 ± 0.5°C). We constructed ensemble waveforms from 15–25 individual sweeps and digitally leak subtracted them using scaled versions of the steps to –70 mV. We filtered the recordings at 2 kHz (8-pole Bessel), sampled them at 10 kHz at 16-bit resolution (ITC18, Instrutech Corporation, Port Washington, New York) and stored them on a computer (Apple Computer, Cupertino, California) for offline analysis.

To construct activation curves, we held patches at –100 mV and stepped them to –70, –60, –50, –45, –40, –30, –20, –10 and 0 mV. The peak current at each potential was then converted to a chord conductance assuming a Na^+ reversal potential of +55 mV. We made a least-squares fit to a single Boltzmann function (Mathematica, Wolfram Research, Champaign, Illinois) for each individual patch, yielding a half activation ($V_{1/2}$) and a slope. Somatic patches included K^+ channel blockers to block the fast transient K^+ currents. We included axonal and initial segment patches without blockers in the analysis because they lacked the fast transient current, and the relatively small sustained current reached a maximum well after the peak of the Na^+ current. We included K^+ channel blockers in some patches ($n = 2$ in the axon, $n = 3$ in the initial segment). For inactivation curves, we held patches at potentials between –100 and –30 mV for 3 s and then stepped them to 0 mV to evoke currents. We normalized data to the maximum current (from –100 mV) and fit them to a negative Boltzmann curve. We determined significance by an ANOVA, with a *post hoc* Tukey's test between groups. Statistical significance was taken to be $P < 0.05$. We reported all summary data as mean ± s.e.m.

We made computer simulations using NEURON[40]. The model was similar to that described in Hoffman *et al.*[9] with some modifications. We visualized a layer 5 pyramidal neuron from a 23-day-old rat using biocytin as previously described[23] and reconstructed it morphologically using Neurolucida (MicroBrightfield, Colchester, Vermont). Simulations assumed a temperature of 23°C. Passive parameters were $R_m = 50{,}000\ \Omega cm^2$, $R_i = 100\ \Omega cm$ and $C_m = 1\ \mu F/cm^2$, except in the dendrites, where $C_m = 2\ \mu F/cm^2$. The baseline channel densities were $\bar{g}_{Na} = 0.0336\ S/cm^2$, $\bar{g}_{K(DR)} = 0.0154\ S/cm^2$ and $\bar{g}_{K(A)} = 0.0031 + 0.00465 \times$ (distance from soma per 200 μm). The Na^+ channel density in the axon beyond the initial segment was set threefold higher. The Na^+ channel model was of the form $g_{Na} = \bar{g}_{Na}\, m^3h$. Parameters were determined by least-squares fit to axonal Na^+ current ensemble averages. The maximum value of m^3h was 0.35, and thus the peak Na^+ conductance in the model was about 12 mS/cm^2. Steady-state values for m and h were of the form $ss(v) = \alpha(v)/(\alpha(v) + \beta(v))$, and time constants $\tau = 1/(\alpha(v) + \beta(v))$, $\alpha_m(v) = 0.182(v - V)/(1 - \exp[-\{v - V\}/6])$ and $\beta_m = 0.124(-v + V)/(1 - \exp[\{-v + V\}/6])$, $\alpha_h(v) = -0.015(v - V_h)/(1 - \exp[\{v - V_h\}/6])$ and $\beta_h = -0.015(-v + V_h)/(1 - \exp[\{-v + V_h\}/6])$. In the soma, dendrites and initial segment, V was –40 mV. To test the effect of altering the voltage dependence of activation, we varied V between –40 and –48 mV. We used a V of –40 mV across the cell in simulations that varied the initial segment density. We set V_h to –69 mV in the axon and –66 mV in the remainder of the neuron. To allow for errors in estimating the actual length of the initial segment, simulations tested lengths of both 30 and 50 μm. Action potential threshold was taken as the point where the second time derivative of the membrane potential waveform reached a value of $5\ mV/ms^2$.

Acknowledgments

This work was supported by a National Institute of Neurological Disorders and Stroke (NINDS) grant (NS36982) to C.M.C. We thank J. Stringer, D. Johnston, M. Rea, A. Eskin, G. Cahill and S. Dryer for reading earlier versions of the manuscript, and L. Cleary for the use of the Neurolucida system.

Competing interests statement

The authors declare that they have no competing financial interests.

RECEIVED 12 NOVEMBER 2001; ACCEPTED 28 MARCH 2002

1. Mel, B. W. Information processing in dendritic trees. *Neural Comput.* **6**, 1031–1085 (1994).
2. Koch, C. *Biophysics of Computation: Information Processing in Single Neurons* (Oxford Univ. Press, New York, 1999).
3. Shadlen, M. N. & Newsome, W. T. The variable discharge of cortical neurons: implications for connectivity, computation, and information coding. *J. Neurosci.* **18**, 3870–3896 (1998).
4. Regehr, W. G. & Armstrong, C. M. Where does it all begin? *Curr. Biol.* **4**, 436–439 (1994).
5. Adams, P. R. The platonic neuron gets the hots. *Curr. Biol.* **2**, 625–627 (1992).
6. Svoboda, K., Denk, W., Kleinfeld, D. & Tank, D. W. *In vivo* dendritic calcium dynamics in neocortical pyramidal neurons. *Nature* **385**, 161–165 (1997).
7. Turner, R. W., Meyers, D. E. R., Richardson, T. L. & Barker, J. L. The site for initiation of action potential discharge over the somatodendritic axis of rat hippocampal CA1 pyramidal neurons. *J. Neurosci.* **11**, 2270–2280 (1991).
8. Andreasen, M. & Lambert, J. D. C. Regenerative properties of pyramidal cell dendrites in area CA1 of the rat hippocampus. *J. Physiol. (Lond.)* **483**, 421–441 (1995).
9. Hoffman, D. A., Magee, J. C., Colbert, C. M. & Johnston, D. K^+ channel regulation of signal propagation in dendrites of hippocampal pyramidal neurons. *Nature* **387**, 869–875 (1997).
10. Stuart, G., Schiller, J. & Sakmann, B. Action potential initiation and propagation in rat neocortical pyramidal neurons. *J. Physiol. (Lond.)* **505**, 617–632 (1997).
11. Spruston, N., Schiller, Y., Stuart, G. & Sakmann, B. Activity-dependent action potential invasion and calcium influx into hippocampal CA1 dendrites. *Science* **268**, 297–300 (1995).
12. Moore, J. W. & Westerfield, M. Action potential propagation and threshold parameters in inhomogeneous regions of squid axon. *J. Physiol. (Lond.)* **336**, 285–300 (1983).
13. Moore, J. W., Stockbridge, N. & Westerfield, M. On the site of impulse initiation in a neurone. *J. Physiol. (Lond.)* **336**, 301–311 (1983).
14. Luscher, H. R. & Larkum, M. E. Modeling action potential initiation and back-propagation in dendrites of cultured rat motoneurons. *J. Neurophysiol.* **80**, 715–729 (1998).
15. Farinas, I. & DeFelipe, J. Patterns of synaptic input on corticocortical and corticothalamic cells in the cat visual cortex II. The axon initial segment. *J. Comp. Neurol.* **304**, 70–77 (1991).
16. Palay, S. L., Sotelo, C., Peters, A. & Orkland, P. M. The axon hillock and the initial segment. *J. Cell Biol.* **37**, 193–201 (1968).
17. Dodge, F. A. & Cooley, J. W. Action potential of the motoneuron. *IBM J. Res. Dev.* **17**, 219–229 (1973).
18. Mainen, Z. F., Joerges, J., Huguenard, J. R. & Sejnowski, T. J. A model of spike initiation in neocortical pyramidal neurons. *Neuron* **15**, 1427–1439 (1995).
19. Rapp, M., Yarom, Y. & Segev, I. Modeling back propagating action potential in weakly excitable dendrites of neocortical pyramidal cells. *Proc. Natl. Acad. Sci. USA* **93**, 11985–11990 (1996).
20. Catterall, W. A. Localization of sodium channels in cultured neural cells. *J. Neurosci.* **1**, 777–783 (1981).
21. Angelides, K. J., Elmer, L. W., Loftus, D. & Elson, E. Distribution and lateral mobility of voltage-dependent sodium channels in neurons. *J. Cell Biol.* **106**, 1911–1924 (1988).
22. Alessandri-Haber, N. *et al*. Specific distribution of sodium channels in axons of rat embryo spinal motoneurones. *J. Physiol. (Lond.)* **518**, 203–214 (1999).
23. Colbert, C. M. & Johnston, D. Axonal action-potential initiation and Na^+ channel densities in the soma and axon initial segment of subicular pyramidal neurons. *J. Neurosci.* **16**, 6676–6686 (1996).
24. Stuart, G. J. & Sakmann, B. Active propagation of somatic action potentials into neocortical pyramidal cell dendrites. *Nature* **367**, 69–72 (1994).
25. Rasband, M. N., Trimmer, J. S., Peles, E., Levinson, S. R. & Shrager, P. K^+ channel distribution and clustering in developing and hypomyelinated axons of the optic nerve. *J. Neurocytol.* **28**, 319–331 (1999).
26. Golding, N. L. & Spruston, N. Dendritic sodium spikes are variable triggers of axonal action potentials in hippocampal CA1 pyramidal neurons. *Neuron* **21**, 1189–1200 (1998).
27. Kloosterman, F., Peloquin, P. & Leung, L. S. Apical and basal orthodromic population spikes in hippocampal CA1 *in vivo* show different origins and patterns of propagation. *J. Neurophysiol.* **86**, 2435–2444 (2001).
28. Carras, P. L., Coleman, P. A. & Miller, R. F. Site of action potential initiation in amphibian retinal ganglion cells. *J. Neurophysiol.* **67**, 292–304 (1992).
29. Zecevic, D. Multiple spike-initiation zones in single neurons revealed by voltage-sensitive dyes. *Nature* **381**, 322–325 (1996).
30. Edwards, E. & Ottoson, D. The site of impulse initiation in a nerve cell of a crustacean stretch receptor. *J. Physiol. (Lond.)* **143**, 138–148 (1958).
31. Gogan, P., Gueritaud, J. P. & Tyc-Dumont, S. Comparison of antidromic and orthodromic action potentials of identified motor axons in the cat's brain stem. *J. Physiol. (Lond.)* **335**, 205–220 (1983).
32. Chavez-Noriega, L. E., Halliwell, J. V. & Bliss, T. V. P. A decrease in firing threshold observed after induction of the EPSP-spike (E-S) component of long-term potentiation in rat hippocampal slices. *Exp. Brain Res.* **79**, 633–641 (1990).
33. Astman, N., Gutnick, M. J. & Fleidervish, I. A. Activation of protein kinase C increases neuronal excitability by regulating persistent Na^+ current in mouse neocortical slices. *J. Neurophysiol.* **80**, 1547–1551 (1998).
34. Matsumoto, E. & Rosenbluth, J. Plasma membrane structure at the axon hillock, initial segment and cell body of frog dorsal root ganglion cells. *J. Neurocytol.* **14**, 731–747 (1985).
35. Stuart, G., Spruston, N., Sakmann, B. & Hausser, M. Action potential initiation and backpropagation in neurons of the mammalian CNS. *Trends Neurosci.* **20**, 125–131 (1997).
36. Magee, J. C. Dendritic hyperpolarization-activated currents modify the integrative properties of hippocampal CA1 pyramidal neurons. *J. Neurosci.* **18**, 7613–7624 (1998).
37. Johnston, D., Magee, J. C., Colbert, C. M. & Christie, B. R. Active properties of neuronal dendrites. *Annu. Rev. Neurosci.* **19**, 165–186 (1996).
38. Buhl, E. H. *et al.* Physiological properties of anatomically identified axo-axonic cells in the rat hippocampus. *J. Neurophysiol.* **71**, 1289–1307 (1994).
39. Cobb, S. R., Buhl, E. H., Halasy, K., Paulsen, O., & Somogyi, P. Synchronization of neuronal activity in hippocampus by individual GABAergic interneurons. *Nature* **378**, 75–78 (1995).
40. Hines, M. NEURON—a program for simulation of nerve equations. in *Neural Systems: Analysis and Modeling* (ed. Eeckman, F.) 127–136 (Kluwer, Norwell, Massachusetts, 1993).

errata

Prefontal cortex in long-term memory: an "interference" approach using magnetic stimulation

Simone Rossi, Stefano F. Cappa, Claudio Babiloni, Patrizio Pasqualetti, Carlo Miniussi, Filippo Carducci, Fabio Babiloni and Paolo M. Rossini
Nat. Neurosci. **4**, 948–952 (2001)

The title of this article contained a typographical error. It should have read as follows:

Prefrontal cortex in long-term memory: an "interference" approach using magnetic stimulation

Ion channel properties underlying axonal action potential initiation in pyramidal neurons

Costa M. Colbert and Enhui Pan
Nat. Neurosci. **5**, 533–538 (2002)

A printer's error introduced an extraneous diagonal line into Fig. 2b on page 534. The correct figure is reproduced below.

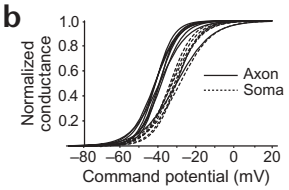

Fig. 2. Na^+ channel properties differ between the soma and axon. (**b**) Voltage dependence of activation in somatic and axonal patches. Each curve is the best-fit Boltzmann for an individual patch. Axonal Na^+ channels (solid lines) were activated by less depolarization than somatic channels (dotted lines).

corrigenda

Neurotrophins use the Erk5 pathway to mediate a retrograde survival response

Fiona L. Watson, Heather M. Heerssen, Anita Bhattacharyya, Laura Klesse, Michael Z. Lin and Rosalind A. Segal
Nat. Neurosci. **4**, 981–988 (2001)

In Fig. 5e on page 986, the pluses and minuses for lines "PD to DA" and "PD to CB" were incorrect. The conclusions stated in the text and the experimental description in the figure legend were correct. The corrected figure is reproduced below.

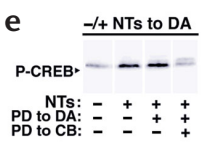

Fig. 5. Activation of Erk5 promotes survival. (**e**) Neurons in compartmented cultures were treated with PD98059 (PD) to distal axons or cell bodies, as indicated. Distal axons were stimulated with neurotrophins and cell body lysates were immunoblotted for P-CREB. PD treatment of distal axons alone does not prevent CREB phosphorylation. When PD is applied to the cell bodies, CREB phosphorylation is inhibited.

A-kinase anchoring proteins in amygdala are involved in auditory fear memory

Marta A.P. Moita, Raphael Lamprecht, Karim Nader and Joseph E. LeDoux
Nat. Neurosci. **5**, 837–838 (2002)

The authors wish to correct their supplementary methods online, which gave the wrong sources for three antibodies. The mouse anti-RIIα and anti-RIIβ antibodies were obtained from Transduction Laboratories (San Diego, California), and the rabbit anti-AKAP150 antibody was obtained from Santa Cruz Biotechnology (Santa Cruz, California).